Available online at www.sciencedirect.com
SCIENCE DIRECT
Hearing Research 215 (2006) 84–96
Hearing Research
www.elsevier.com/locate/heares

Research paper

A study of hearing aid gain functions based on a nonlinear nonlocal feedforward cochlea model

Yongsam Kim [a], Jack Xin [b,c,*], Yingyong Qi [d]

[a] *Institute of Computational Engineering and Sciences (ICES), University of Texas at Austin, Austin, TX 78712, USA*
[b] *Department of Mathematics, UC Irvine, Irvine, CA 92697, USA*
[c] *ICES, University of Texas at Austin, Austin, TX 78712, USA*
[d] *Qualcomm Inc., 5775 Morehouse Drive, San Diego, CA 92121, USA*

Received 13 November 2005; received in revised form 13 March 2006; accepted 14 March 2006
Available online 6 May 2006

Abstract

A model based sound amplification method is proposed and studied to enhance the ability of the hearing impaired. The model consists of mechanical equations on basilar membrane and outer hair cell (OHC). The OHC is described by a nonlinear nonlocal feedforward model. In addition, a perceptive correction is defined to account for the lumped effect of higher level auditory processing, motivated by the intelligibility function of the hearing impaired. The gain functions are computed by matching the impaired model output to the perceptively weighted normal output, and qualitative agreement is achieved with NAL-NL1 prescription on clean signals. For noisy signals, an adaptive gain strategy is proposed based on the signal to noise ratios (SNR) computed by the model. The adaptive gain functions provide less gain as SNRs decrease so that the intelligibility can be higher with the adaptivity.

Keywords: Cochlea model; Intelligibility; Model based amplification; Noises; Adaptive amplification

1. Introduction

Sound amplification in hearing aids for impaired ears is a fascinating problem that has been largely studied by empirical methods (Dillon, 2001; Killion, 1996; Ching et al., 2001 and references therein). In National Acoustic Labs, Nonlinear Version 1 (NAL-NL1) strategy (Ching et al., 2001; Acoustic Labs and NAL-NL1 software, 2003), a speech intelligibility (SI) function is defined over a number of frequency bands based on empirical functions (e.g., effective and desensitized audibility) and hearing loss audiogram. The input sound is amplified to maximize SI while keeping loudness no more than what is perceived by a normal ear.

In this paper, we develop a model based approach by combining the peripheral mechanical output in the inner ear (cochlea) with a perceptive correction accounting for the lumped effect of higher auditory pathways. The correction adapts the effective audibility function of NAL-NL1, and measures the proportion of intelligible information in each frequency band for the impaired ear to attain by amplification. A nonlinear nonlocal cochlea model parametrized by the outer hair cell (OHC) activity is presented and shown to capture compression, suppression and frequency selectivity. By a proper choice of OHC active parameter, the model can play the role of a normal ear or an impaired ear with severe, moderate and mild loss.

Abbreviations: BM, basillar membrane; OHC, outer hair cell; NAL-NL1, National Acoustic Labs, Nonlinear Version 1; SI, speech intelligibility; SNR, signal to noise ratio; 2D, two-dimensional; ms, millisecond; CP, characteristic place; SPL, sound pressure level; dB, decibel; HL, hearing loss; nm, nanometer; kHz, kilo-Hertz; SII, speech intelligibility index; LDF, level distortion factor; ITR, Information Technology Research; ICES, Institute of Computational Engineering and Sciences

* Corresponding author. Address: Department of Mathematics, UC Irvine, Irvine, CA 92697, USA. Tel.: +1 949 824 5309; fax: +1 949 824 7993.
E-mail addresses: kimy@ices.utexas.edu (Y. Kim), jxin@math.uci.edu (J. Xin).

0378-5955/$ - see front matter
doi:10.1016/j.heares.2006.03.013

It is well known (Moore, 2000; Geisler, 1998) that the reduced OHC motility is one of the common causes of sensorineural hearing loss. Such hearing loss raises hearing thresholds, broadens tuning curves, and reduces dynamic range. Our strategy consists of comparing the impaired and normal model outputs, then finding a gain value to the input sound so that the impaired output matches a weighted (perceptively corrected) normal output. This is partially motivated by a recent NAL finding (Ching et al., 2001) that amplification in the high frequency range only to offset the loss may reduce the intelligibility. Qualitative agreement with NAL-NL1 will be shown.

Our model based method is simpler than the empirical method (Ching et al., 2001) in that there are fewer number of fitting parameters, and smaller ranges of parameter variation. Partly this is because, in the first step, the model has approximated certain nonlinear aspects of hearing such as nonlinear compression and frequency tuning, so less parameter adjustment is needed in the second correction step. Moreover, the model based approach is robust enough to extend to gain computation for signals in noisy environment, for which an empirical method has not been available. We computed adaptive gains with the help of model estimated signal to noise ratios for broad band, low and high frequency noises. As long been noticed by the users, noises have dramatic effects on the performance of hearing aids. The adaptive gains show the noise effect on the gain functions in a transparent and quantitative manner.

The paper is organized as follows. In Section 2, a two-dimensional cochlea model with a feedforward OHC module is described. In Section 3, the model is shown to generate salient features of normal and impaired ears. In Section 4, NAL-NL1 intelligibility and audibility functions are reviewed and their properties illustrated. Then our model based method of gain amplification is given. Comparison of our method with NAL-NL1 is made. Adaptive gain strategy is presented along with a model based SNR calculation. The effects of different types of noises on the gain curves are illustrated and compared. Such noises include broad band, low (high) frequency banded and realistic road noises. The overall gains are reduced as a result of noise interference, with the amount of reduction dependent on the relative intensities and frequency contents of the signals and noise. The discussions and conclusions are in Section 5.

2. Nonlinear nonlocal feedforward model

The normal and impaired ear functions are modeled by a coupled BM and OHC system of equations based on mechanics and neurophenomenology. The cochlea contains an elastic structure, basilar membrane (BM), which is immersed in an incompressible Stokes fluid (Leveque et al., 1988; Neely, 1985). The longitudinal cross-section of the upper cochlea chamber is simplified into a 2-dimensional (2D) rectangle $\Omega = [0, L] \times [0, H]$, with BM at the bottom $z = 0$, see the top panel of Fig. 1. The lower cochlea chamber is symmetric with respect to $z = 0$, and the fluid flow is inviscid and irrotational. The pressure difference drives BM into motion, see the solid line in the figure for

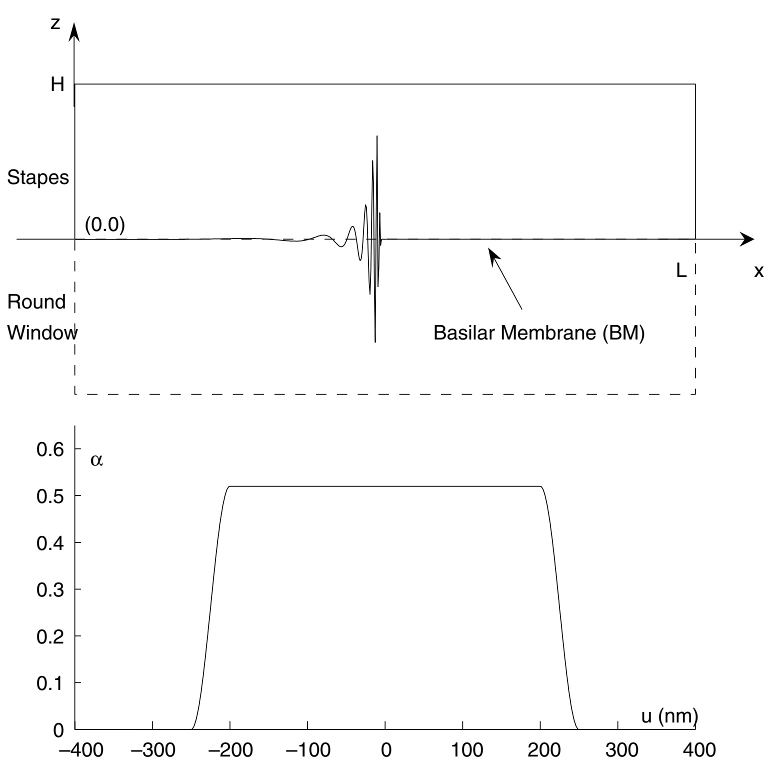

Fig. 1. Illustration of 2D cochlea model on basilar membrane (top), and the variation of the local gain factor α vs. the BM displacement u (bottom).

a BM displacement during its evolution under a steady tonal input. The BM displacement is scaled up by several orders of magnitude to better illustrate a typical BM response to a single tone. The sensitivity of BM is controlled by a feedforward model of outer hair cells (OHC), (Kim and Xin, 2005; Lim, 2000; Lim and Steele, 2002).

Let $p(x,z,t)$ be the fluid pressure in the cochlea, $u(x,t)$ the vertical displacement of BM, $q(x,t)$ the OHC force on BM. The model equations are:

$$\left(\frac{\partial^2}{\partial x^2}+\frac{\partial^2}{\partial z^2}\right)p(x,z,t)=0, \quad (x,z)\in[0,L]\times[0,H], \tag{1}$$

$$p(L,z,t)=0, \quad \frac{\partial p}{\partial x}(0,z,t)=2\rho T_m p_e(t), \quad 0\leqslant z\leqslant H, \tag{2}$$

$$\frac{\partial p}{\partial z}(x,H,t)=0, \quad \frac{\partial p}{\partial z}(x,0,t)=2\rho u_{tt}(x,t), \quad 0\leqslant x\leqslant L, \tag{3}$$

$$q(x,t)+p(x,0,t)=Mu_{tt}+R(x)u_t+S(x)u, \quad 0\leqslant x\leqslant L, \tag{4}$$

$$q(x+\Delta,t)=\alpha(x,u,t)(p(x,0,t)+q(x,t)), \tag{5}$$

where $p_e(t)$ is input sound pressure at the ear drum; T_m is a bounded linear mapping from the pressure p_e to the stapes acceleration, mimicking the middle ear filtering (see Kim and Xin, 2005 for details); ρ and M are constant densities of the fluid and BM, respectively. The function $R(x)$ denotes the BM damping per unit length:

$$R(x)=0.25\exp(-1.2x)+0.018. \tag{6}$$

The BM stiffness function $S(x)$ based on the data (Greenwood, 1990) is:

$$S(x)=4\pi^2 M(0.1654\exp(4.83(1-x/L))-0.8)^2. \tag{7}$$

Table 1 tabulates physical and numerical parameters (ms short for millisecond).

In Eqs. (4) and (5), $q(x,t)$ is the amplification force generated from OHC. While it is created at location x along BM, it acts at a point $x+\Delta$ downstream on BM due to the longitudinal tilt of OHC (see Eq. (5)). For more details on this OHC mechanical property (see Lim, 2000; Lim and Steele, 2002). The OHC force, however, is known to saturate as the BM displacement increases in magnitude (Geisler, 1998; Pickles, 1988). In Lim (2000) and Lim and Steele (2002), the gain factor α depends on the BM displacement u, with the profile shown in the bottom of Fig. 1. The gain factor α remains fairly constant for small BM displacement and tapers off to zero as the BM displacement increases. In time domain computations, the local nonlinear form of the gain may lead to sawtooth-shaped gain and the unstable motion of BM. In Kim and Xin (2005), a nonlocal form of the gain factor is introduced to remove the instability. The nonlocal form is also supported by recent physiological findings (de Boer and Nuttall, 2003). The resulting solutions are stable in time (Kim and Xin, 2005). Let $g(u)$ be the nonlinear function shown in Fig. 1, the nonlocal nonlinear gain factor $\alpha(x,u,t)$ is:

$$\alpha(x,u,t)=\frac{\gamma}{\sqrt{\lambda\pi}}\int_0^L \exp(-(x-x')^2/\lambda)g(u(x',t))\,dx', \tag{8}$$

where γ and λ are constants. The parameter γ controls the size of the gain factor, and $\sqrt{\lambda}$ gives the BM length scale where the gain is effective.

The feedforward model of OHC (5) has been studied recently by Lim (2000) and Lim and Steele (2002), as a faithful micro-mechanical description of OHC dynamics. Nonlinear phenomena such as compression and tonal suppression are accurately recovered by the model when coupled to macromechanical equations (Lim, 2000; Lim and Steele, 2002; Kim and Xin, 2005). The model has a wide dynamic range of responses especially in the high frequency range and so is quite suitable for our purpose of studying high frequency hearing loss. The feedforward model is thus selected based on its wide dynamic range and mathematical simplicity.

The Eqs. (1)–(5) are solved with an efficient and accurate numerical scheme (Kim and Xin, 2005). A boundary integral approach is used to express the pressure p as a functional of u, and restrict p on the BM so that the reduced equations are defined entirely on the BM. A second-order accurate discretization method is applied in both space and time, together with an iterative solver to invert mass matrix and advance solutions at each time step. The resulting numerical solutions have been shown to capture common ear responses such as compression, tone or noise suppression. We refer to Kim and Xin (2005) for details on model calibration and numerical accuracy. Numerical grid sizes are listed in Table 1.

3. Normal and impaired ears

Let us show that our model captures the known behaviors of normal and impaired ears with suitable choice of parameters. The OHC tilt Δ is 0.005 cm, same as the meshwidth Δx. For a normal ear, we choose $\gamma=0.52$ in Eq. (8). For ears with hearing loss, γ is smaller or may even be zero. Larger γ or α implies that BM responses are more amplified and more nonlinear for strong enough sound input. For both normal and impaired ears, $\lambda=0.01$ cm^2.

It is known that defects in hair cell functions may cause both raised hearing threshold and loudness recruitment (Killion, 1996; Oxenham and Bacon, 2003). Fig. 2 shows the model output (amplitude of BM displacement) as a function of the input level in dB (decibel) of sound pressure level (SPL). The input frequency is chosen at 0.5 kHz (left), 2 kHz (middle), and 6 kHz (right), respectively. At each frequency, we compare the outputs of normal ear and

Table 1
Model parameters

Parameters	Symbol	Magnitude	Unit
Membrane density	M	0.05	g/cm^2
Fluid density	ρ	1	g/cm^3
Length of cochlea	L	3.5	cm
Height of cochlea	H	0.1	cm
Meshwidth	Δx	0.005	cm
Time duration	Δt	0.0025	ms

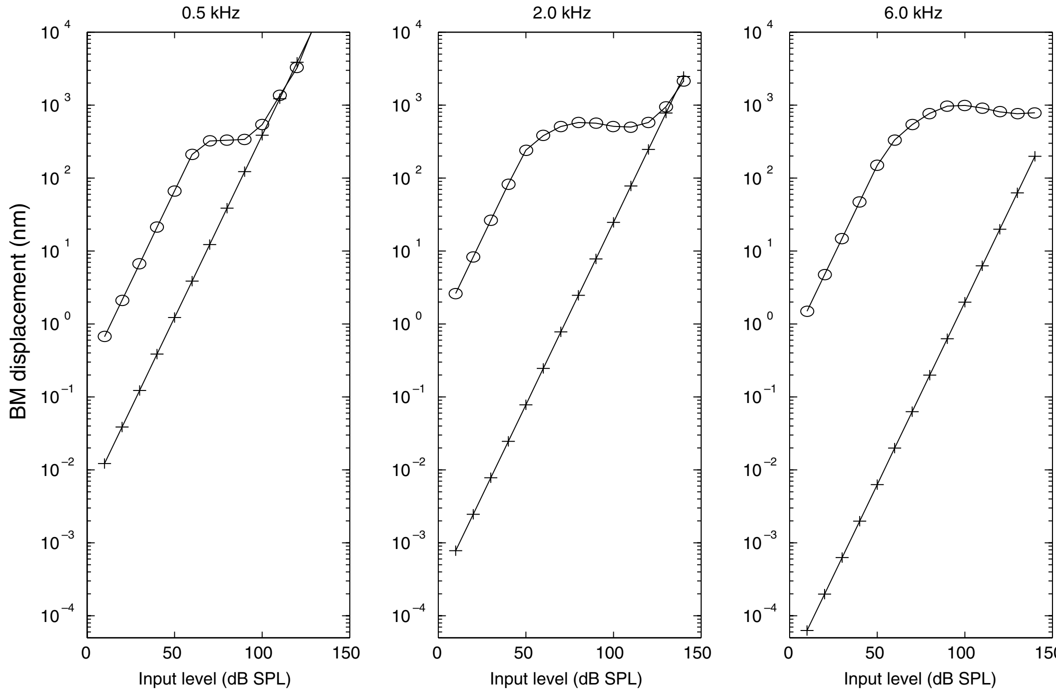

Fig. 2. Output (amplitude of BM displacement) vs. input level (dB) at 0.25 kHz (left), 2 kHz (middle), and 6 kHz (right) for normal (line–circle, $\gamma = 0.52$) and impaired (line–plus, $\gamma = 0$) ears. The impaired ear has raised hearing thresholds, and loses the compressive nonlinearity in a normal ear.

impaired ear. For the impaired ear, the gain constant $\gamma = 0$ and the model is linear (passive). The input level starts at 10 dB. We see that if 1 nm is the BM threshold of hearing, then the impaired ear with $\gamma = 0$ has a higher threshold of sound intensity (dB in SPL). This difference of the hearing threshold can be defined as the hearing loss (HL) of the impaired ear. Here, HLs are 35, 71, and 88 dB at each of the above frequencies. The convergence of response curves at large input levels (100–140 dB SPL) shows the loudness recruitment. In other words, a very loud sound annoying and harmful to a normal ear gives a similar amount of discomfort to an impaired ear (Oxenham and Bacon, 2003).

An impaired ear also suffers from the loss of frequency selectivity. Fig. 3 compares the isodisplacement curves for

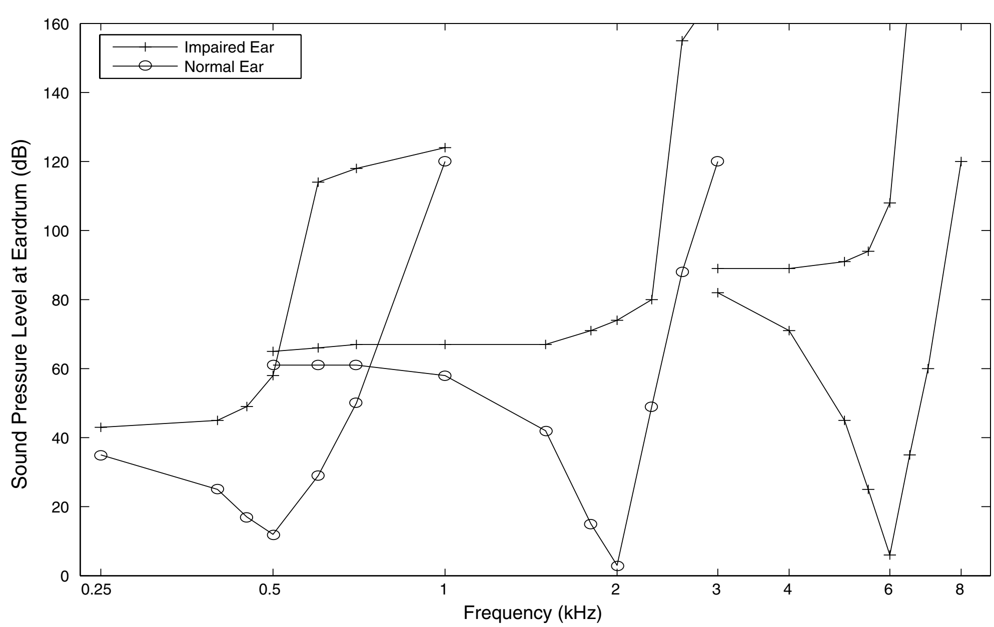

Fig. 3. Isodisplacement (tuning) curves for normal (–o) and impaired (–+) ears. The isodisplacement curves are computed with 1 nm BM displacement as threshold. The curves of normal ear are sharply-tuned and more sensitive around CP. The impaired ear has broadened and raised tuning curves causing poor frequency selectivity.

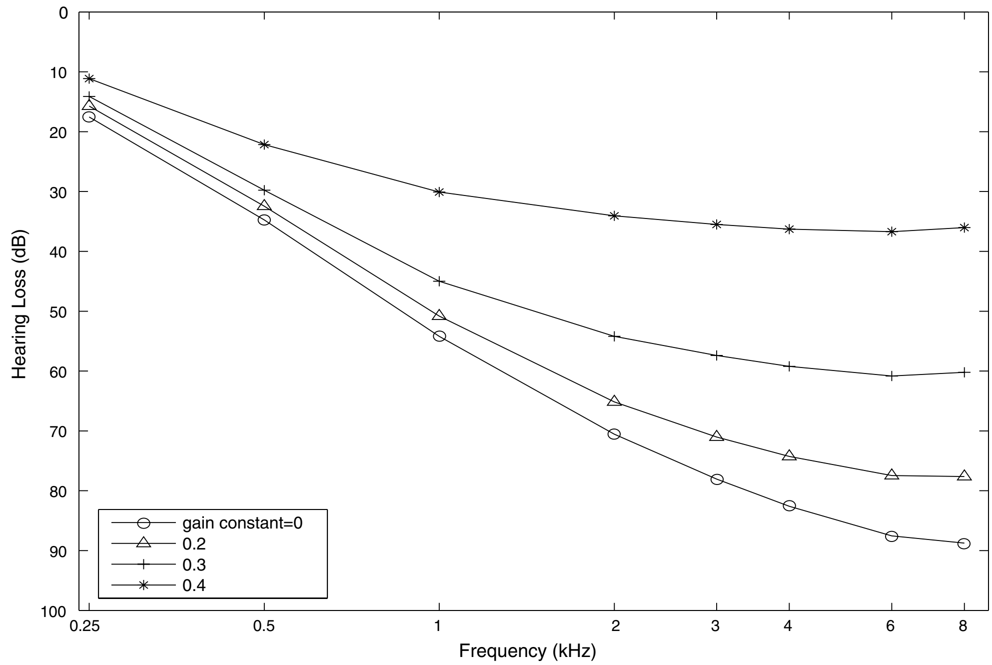

Fig. 4. HL curves for four different impaired ears with four gain constants $\gamma = 0$, 0.2, 0.3, and 0.4. The losses are generally increasing with frequency, typical for OHC related hearing loss.

normal ($\gamma = 0.52$) and impaired ($\gamma = 0.0$) ears. The curves in the figure are obtained as follows. Let the modulus of the BM displacement be $|u| = |u|(x; A_j, f_j)$ where A_j and $f_j (j = 1, \cdots, J)$ are the input frequency and intensity, respectively. We set 1 nm as the threshold value for the BM displacement, then find A_j so that $|u|(x; A_j, f_j) = 1$ nm, for each characteristic place (CP) $x_i = cp(f_i), f_i = 0.5$, 2, and 6 kHz. If f is 2 kHz, for example, $x(f) = 1.61$ cm from the stapes. Fig. 3 represents plots of A_j as a function of f_j for each $i = 1, 2, 3$, and $\gamma = 0.52$ and 0.0. The curves in line–circle are for the normal ear, and have lower and sharper tips. The plus–line curves are for the impaired ear, and they are raised and broadened. The experiments on animal cochlea (Robles and Ruggero, 2001; Ruggero et al., 1997) show similar properties.

Our model yields a much broader range of OHC gain at high frequencies than at low frequencies. The difference of model responses in dB scale between normal and impaired ears for pure tone input at absolute hearing threshold levels is referred to as hearing loss (HL). Fig. 4 shows four different HL curves at $\gamma = 0$, 0.2, 0.3, and 0.4. The shape of these HL curves are typical for OHC induced hearing loss. Severe loss at low frequencies may come from other sources such as inner hair cells (Moore, 2000).

4. Model based amplification

We present a scheme to simulate hearing aid amplification by combining the peripheral ear model above and a correction step mimicking higher level auditory processing. The correction step is based on speech intelligibility (SI) and the resulting gain functions will be compared with those from NAL-NL1, which is introduced by the National Acoustic Laboratories in Australia and widely used as a prescription strategy for nonlinear hearing aids.

The design strategy of NAL-NL1 is to amplify sound to an impaired ear so as to maximize SI while keeping the loudness no greater than what is perceived by a normal ear (Ching et al., 2001). We shall first review the SI functions used by NAL-NL1 and study their properties, then present our formula for amplification, as a simplification and an alternative strategy.

4.1. Effective audibility and intelligibility

The speech intelligibility index (SII) is an approximation of speech understanding. Frequency may be divided into eight bands with center frequencies and hearing thresholds as shown in Table 2. In the i-th band, let e_i be the weighting factor, K_i the proportion of audible speech, and L_i the level distortion factor (LDF). Then the audibility A_i and SII are defined as ANSI (1997):

$$\mathrm{SII} = \sum_{i=1}^{8} e_i A_i = \sum_{i=1}^{8} e_i K_i L_i, \quad (9)$$

where L_i accounts for the deterioration of intelligibility with the increase of the input sound level:

$$L_i = \min\left(1, 1 - \frac{E_i' - U_i - 10}{160}\right), \quad (10)$$

where E_i' is the equivalent speech spectrum level and U_i is the standard speech spectrum level for normal vocal efforts,

Table 2
Frequency bands, band center frequencies (kHz), band weights, thresholds (dB), U (dB) and v values

Band i	1	2	3	4	5	6	7	8
Frequency f	0.25	0.5	1	2	3	4	6	8
Weight e_i	0.0261	0.0557	0.0557	0.0557	0.0557	0.0557	0.343	0.011
Threshold	14.07	9.978	7.090	3.2855	−1.004	1.0269	6.1943	9.1996
Standard U	34.75	34.27	25.01	17.32	12.0	9.33	3.0	1.13
$v_{3,i}$	5.0346	5.0402	5.0481	5.0582	5.0638	5.0623	5.0623	5.0623
$v_{4,i}$	0.4167	0.3619	0.2851	0.1864	0.1316	0.0877	0.0877	0.0877
$v_{5,i}$	4.4388	4.4415	4.4453	4.4502	4.4529	4.4550	4.4550	4.4550
$v_{6,i}$	−0.140	−0.099	−0.042	0.0325	0.0736	0.1065	0.1065	0.1065

see Table 2 and also ANSI (1997). The E'_i is the sum of measured speech spectrum and the insertion gain in the band i. The SII is a weighted sum of the audibility at each frequency band (ANSI, 1997), and ranges between 0 (no understanding) and 1 (perfect understanding).

The NAL findings (Ching et al., 1998, 2001) showed that real scores of speech understanding (percentage correct) can be smaller than that predicted by Eq. (9), especially for severely impaired ears and at high frequencies. Effective audibility A_i^* modifies the audibility function A_i in Eq. (9), and is equal to $K_i^* L_i$ where K_i^* is the so-called desensitized audibility:

$$K_i^*(\mathrm{SL}_i, \mathrm{HL}_i) = \frac{m_i}{\left[1 + \left(\frac{30}{\mathrm{SL}_i}\right)^{p_i}\right]^{1/p_i}}, \tag{11}$$

where SL_i denotes the sensation level, and HL_i the hearing loss in the i-th frequency band. The sensation level (SL) is the input amount exceeding the hearing threshold. The m_i and p_i depend on HL as:

$$m_i = \frac{e^{v_{1,i} - v_{2,i} \times \mathrm{HL}_i}}{1 + e^{v_{1,i} - v_{2,i} \times \mathrm{HL}_i}}, \quad p_i = (v_{3,i} - v_{4,i}) \times \frac{e^{v_{5,i} - v_{6,i} \times \mathrm{HL}_i}}{1 + e^{v_{5,i} - v_{6,i} \times \mathrm{HL}_i}} + v_{4,i}, \tag{12}$$

where HL_i is hearing loss and $v_{j,i}$'s ($j = 3, 4, 5, 6, i = 1, 2, \cdots 8$) are given in Table 2 (reproduced from Ching et al., 2001). The $v_{1,i} = 10.951$ and $v_{2,i} = 0.106$, for $i = 1, 2, \cdots 8$. The equations for effective audibility and the parameters therein were derived from experiments on normal and impaired subjects.

Fig. 5 shows the difference of desensitized audibility in case of (0, 30, 60, 90) dB hearing losses at two frequency bands centered at (2, 4) kHz. When hearing loss is small, amplifying sound to an impaired ear to the same sensation level as the normal ear recovers the audibility at both low and high frequencies. When hearing loss is severe (90 dB), while the amplification at low frequency helps to recover the intelligibility, the benefit of high frequency amplification is much reduced. The NAL-NL1 strategy finds the amplification in each frequency region to maxi-

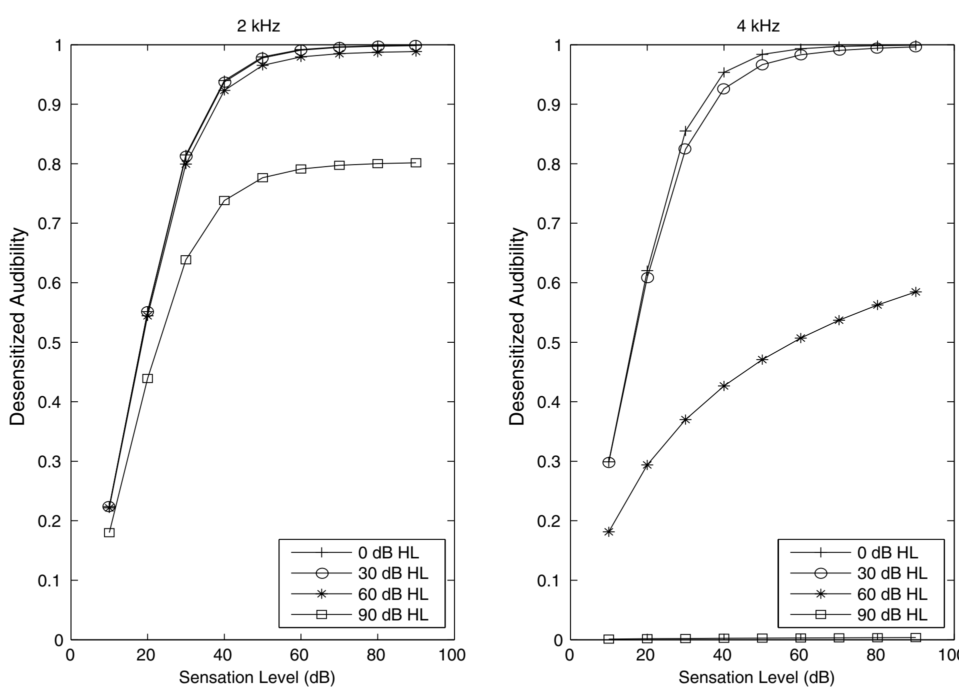

Fig. 5. Desensitized audibility of 0, 30, 60 and 90 dB hearing losses at two frequency bands centered at 2 and 4 kHz. When hearing loss is small, the amplification recovers the audibility of a normal ear at each frequency. When hearing loss is severe, the amplification at low frequency contributes more to the intelligibility than at high frequency where only partial recovery of audibility is possible.

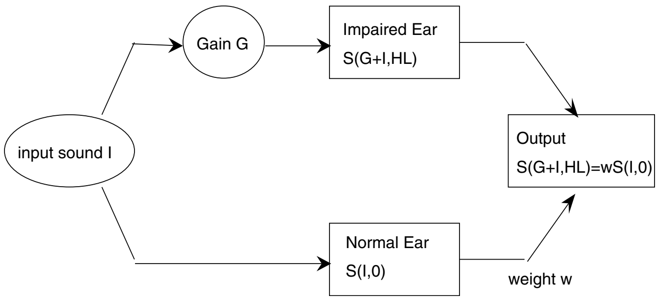

Fig. 6. Flowchart of our method. For a given hearing loss HL at each frequency region, we find the gain function G in terms of input level I such that $S(G+I, \mathrm{HL}) = w(I)S(I, 0)$.

mize the intelligibility function $\mathrm{SII}^* = \sum_{i=1}^{8} e_i K_i^* L_i$ subject to equal loudness of sound (Ching et al., 2001).

Our study proceeds as follows. The normal ear is modeled with $\gamma = 0.52$, and the impaired ear with a smaller value of γ, such as 0, 0.3, 0.4. The model response is the maximum BM displacement denoted by $S_i(I_i, \mathrm{HL}_i)$, where I_i is the input level in dB SPL, and HL_i is the hearing loss of the ear at the i-th frequency band. The input signals are pure tones. Let G_i be the amount of gain to be added to the input signals in the i-th band, then G_i is determined by matching the enhanced impaired response to a weighted normal response:

$$S_i(G_i + I_i, \mathrm{HL}_i) = w_i(I_i)S_i(I_i, 0), \qquad (13)$$

where $w_i(I_i)$ is the weight factor in the i-th band depending on the input level I_i. The $S_i(G_i + I_i, \mathrm{HL}_i)$ is the output of the impaired ear with amplification G_i and $S_i(I_i, 0)$ is the output of the normal ear (zero hearing loss). The weighting factor w_i's form the correction step to account for higher level auditory processing (modification) of peripheral model output. See Fig. 6 for an illustration.

To determine the functional form of w_i's, we adapt the effective audibility functions in NAL and the band importance factors (ANSI, 1997) as:

$$w_i(I_i) = \frac{e_i}{\max(e_i)} \left(\frac{A_i^*(\mathrm{SL}_i, \mathrm{HL}_i)}{A_i^*(\mathrm{SL}_i, 0)} \right)^{a(\mathrm{SL}_i)},$$
$$a(I_i) = 3.6 \times \frac{e^{10-0.11\times\mathrm{SL}_i}}{1 + e^{10-0.11\times\mathrm{SL}_i}}. \qquad (14)$$

Here, the sensation level SL_i is the value of input level I_i subtracted by the hearing threshold level. Since an impaired ear has larger threshold level, it needs a higher input level I_i to reach the same SL_i, which reduces both level distortion factor L_i and A_i^*. The weighting factor w_i measures the defect of an impaired ear to the normal ear. It is an increasing function of the ratio of desensitized audibilities. The amount of increase, however, decreases as the input level goes up, as described in the exponent $a(I_i)$.

The rationale of the matching strategy (13) is this. Because the defect of an impaired ear prevents it from understanding speech as well as a normal ear, the weighted (reduced) output of the normal ear serves as an optimal target for the impaired ear to reach. No gain is needed if the target is below the impaired ear output.

The top of Fig. 7 shows weight functions $w_i(I_i)$ of the input level I_i at the frequencies 2 kHz (left) and 4 kHz (right), with the corresponding HLs being 54 and 61 dB, respectively. The bottom shows two outputs of the normal (○), the impaired (+), and the target output (*) at each input level and frequency. When the input is 4 kHz at 40 dB, for example, the weight is 0.0102. The amplification is determined to equate the aided output of the impaired ear with the target output. The bottom graphs show the amplification geometrically as the lengths (in dB) of the horizontal lines between the target and the impaired output curves.

In Fig. 8, the top represents the hearing loss (audiogram) of an impaired ear with gain factor $\gamma = 0.0$ at each frequency; and the bottom shows the amplification as a function of the input level as is needed for the impaired ear to reach the target output. We observed the wide dynamic range compression. The amplification decreases as the input level increases.

4.2. Comparison with NL1

NAL-NL1, a widely used prescription for nonlinear hearing aids, adopted two concepts: effective audibility and equal loudness. For a given sound or speech, the amplification in each frequency region is determined to maximize the predicted speech intelligibility SII subject to the constraint that the loudness of the sound is no greater than what is perceived by normal people (Ching et al., 1998, 2001). The difference of NAL-NL1 from most of the previous prescription methods is to use effective audibility (desensitized audibility), which approximates better the intelligibility of severely impaired ears. Consequently, in the prescription, the high frequency regions are much less amplified than the middle frequency region.

Fig. 9 compares the prescription results of NAL-NL1 and our method. The left column in each row shows the hearing loss level (HL) for the ear model with gain constant $\gamma = 0$ (top), 0.3 (middle), and 0.4 (bottom), respectively. We regard the first row as from a severely impaired ear, the second from a moderately impaired ear, and the third from a mildly impaired ear. The middle plots in each row are from the prescription of a commercial NAL-NL1 (Acoustic Labs and NAL-NL1 software, 2003). The right column is computed by our method. In both fitting methods, the amplification (gain) needed for each impaired ear is a function of the input frequency. Different curves correspond to different input intensity levels.

When hearing loss is severe and moderate (top and middle), both methods generate compressive wide range gains, i.e., when the input level increases, the amount of amplification decreases. When the sound input level to the severely impaired ears is moderate (below 60 dB), both methods also give the largest gain in the middle frequency region between 2 and 4 kHz which contributes most to the

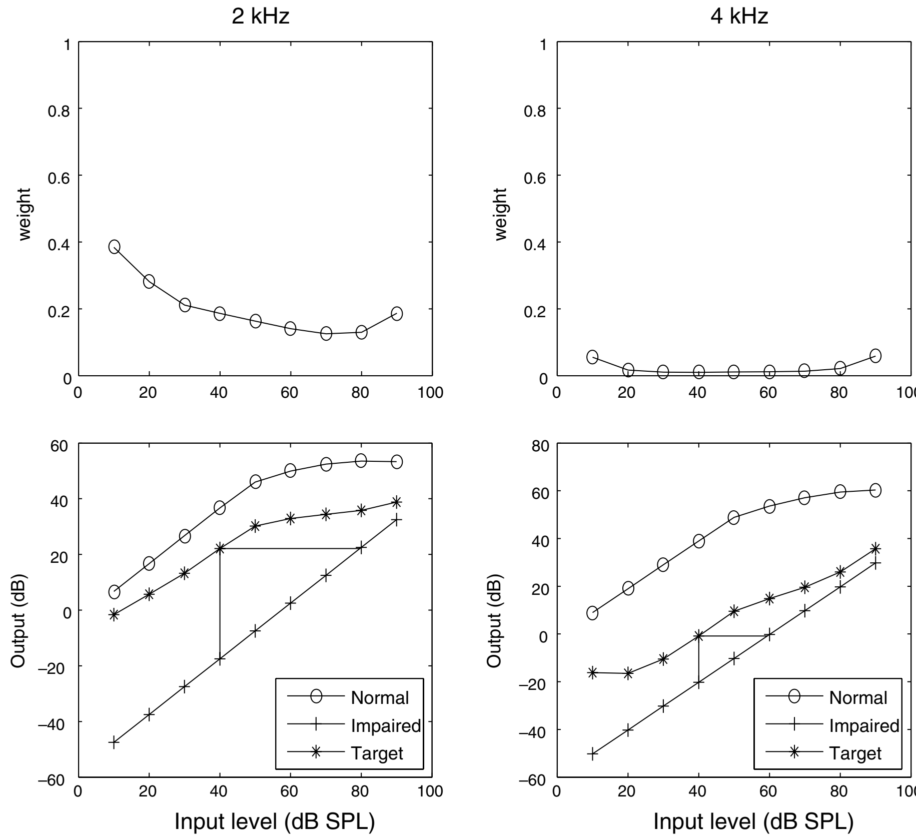

Fig. 7. Top: weight functions $w_i(I_i)$ of input level I_i when the frequencies are 2 kHz (left) and 4 kHz (right) and the corresponding HLs are 54 and 61 dB, respectively. Bottom: Two outputs of normal (○), impaired (+) and the target output (∗) at each input level and frequency. In the right-bottom graph, the amplification of 4 kHz at 40 dB is determined as the length of the horizontal line; no amplification is provided if the target is below the impaired ear response. The reference dB level is the absolute hearing threshold of the normal ear.

intelligibility. We noted that the NAL-NL1 prescription gives no gain near the 8 kHz region. NAL curves do not continue up to 8 kHz in the top frame of the middle column though the numerical gain values are zero there. Yet our method still prescribes some. Overall, our method reaches qualitative agreement with NAL-NL1.

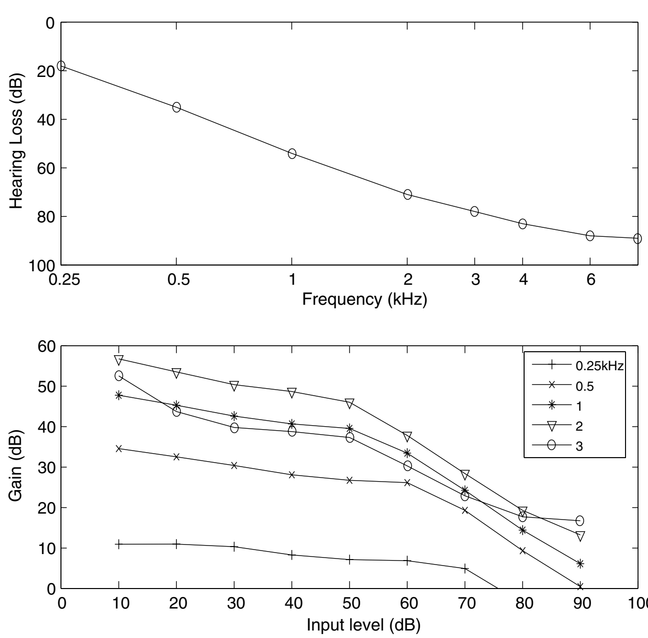

Fig. 8. Hearing loss and amplification. The prescription for the amplification in the bottom shows the wide dynamic range compression.

4.3. Amplification strategy for noisy signals

In this section, we introduce an amplification strategy for impaired ears when the input sound is noisy. In noisy environment, impaired ears often have greater difficulties hearing than normal ears. Blind amplification without considering the noise effects can make the amplified signals even less understandable. An adaptive amplification strategy is to adjust the full amplification for the clean signals based on signal to noise ratios (SNR). Here, we compute SNRs with our model (normal ear, $\gamma = 0.52$) instead of measuring SNR directly from the input signal and noise. This way, we approximate better the perception or understanding.

Let $u_S(x,t)$ and $u_N(x,t)$ be the BM responses of a pure tone S and a noise N, respectively. Let $u_{S+N}(x,t)$ represent the BM response when the input is the mixture of tone S and noise N. The top of Fig. 10 shows the noisy input signal when S is a 2 kHz 40 dB pure tone and N is a 40 dB banded noise with its frequency contents in $[0.5, 8]$ kHz. The bottom graph shows a few overlapped BM responses during the time interval $[29.8, 30]$ ms.

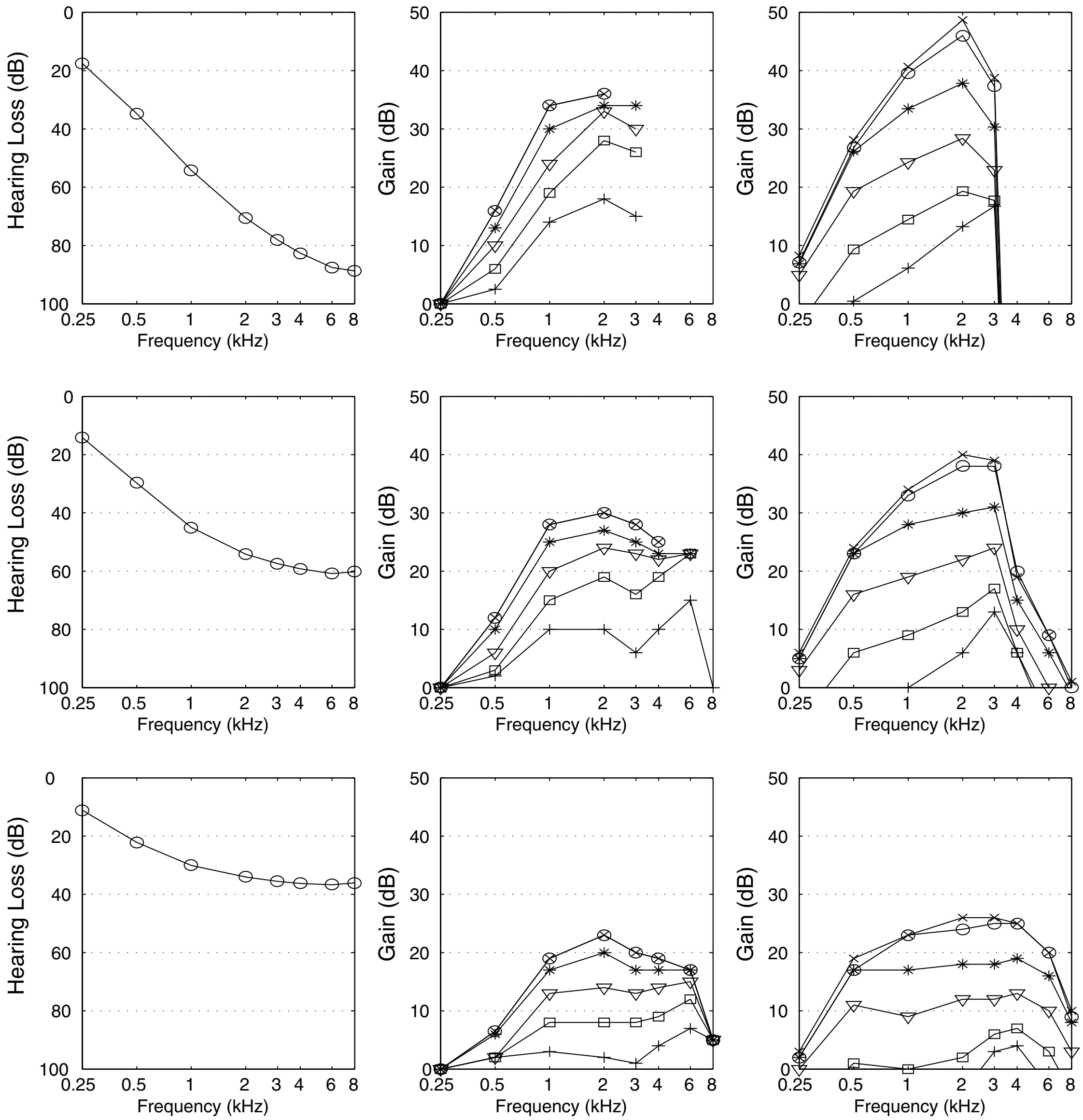

Fig. 9. Comparison between the prescription results of NAL-NL1 (center column) and our method (right column). The gains are plotted as functions of the input tonal frequency, and are labeled with tone dB intensity ($x = 40$, $\bigcirc = 50$, $* = 60$, $\bigtriangledown = 70$, $\square = 80$, and $+ = 90$ dB). Both methods generate compressive wide range hearing aids, and, when the sound input level is moderate (below 60 dB), both give the largest gain in the middle frequency region between 2 and 4 kHz.

For a noisy input sound $J = S + N$, let the model output be $u_J(x, t)$. Define the function $R(u_J(x,t))$:

$$R(u_J(x,t)) = \left(\frac{1}{M \cdot N} \sum_{i=1}^{M} \sum_{j=1}^{N} |u_J(x_i, t_j)|^2 \right)^{1/2}, \tag{15}$$

where x_i's range over $[0, L]$ cm, L the BM length; the t_j's range from t_0 to the final stopping time T. The t_0 is a time after the initial transients have decayed. The $R(u_J(x,t))$ is up to a constant the space–time L^2 norm of the function $u_J(x,t)$.

For given signal S and noise N, its signal-to-noise ratio (SNR) is $20 \log_{10}(I_S/I_N)$ dB where I_S and I_N are the levels of the sound and noise, respectively. This SNR is computed from the input levels. Since ear is nonlinear and compressive, it would be better to measure SNR from output levels along the auditory pathways. Moreover, the deterioration of intelligibility by noise depends on how the frequencies of the noise overlap with those of the signal. It is reasonable to calculate SNR in each frequency band. A noise with frequency content from 4 to 8 kHz, for example, affects most the intelligibility of a sound in the same frequency range, while it affects much less lower frequency sounds. In order to take this effect into account, we divide the BM length into eight partitions each of which has its center frequency $f_i, i = 1, \ldots, 8$, in Table 2. Let $\chi_i(x)$ be the partition function of band i with center frequency f_i, $\sum_{i=1,8} \chi_i(x) = 1$. The frequency bands in Table 2 are first mapped to nonoverlapping intervals on BM (Greenwood, 1990). A partition of unity can then be constructed,

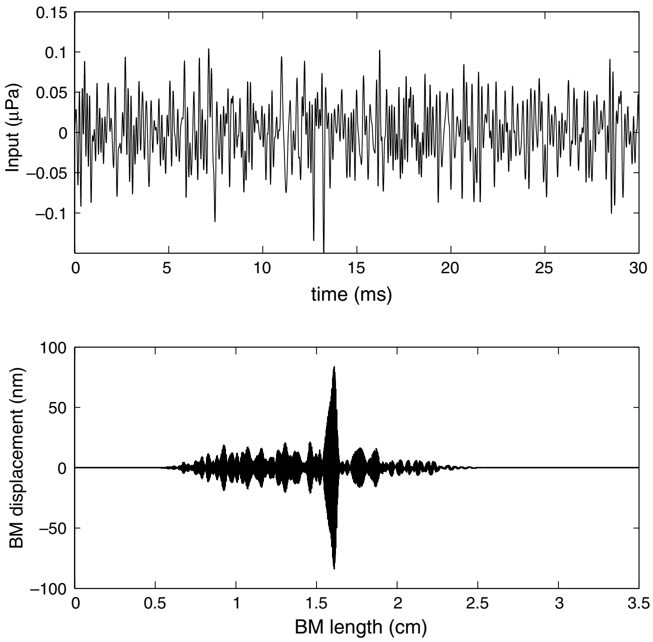

Fig. 10. Input and output of pure tone and noise: The top panel shows the input sound which is the mixture of a pure tone 2 kHz and a noise with its frequency banded in [0.5, 8] kHz, both at 40 dB. The bottom shows a few overlapped BM responses during the time interval [29.8, 30] ms when the input is the one shown in the top panel. The highest peak around 1.6 cm BM length is due to the 2 kHz pure tone input.

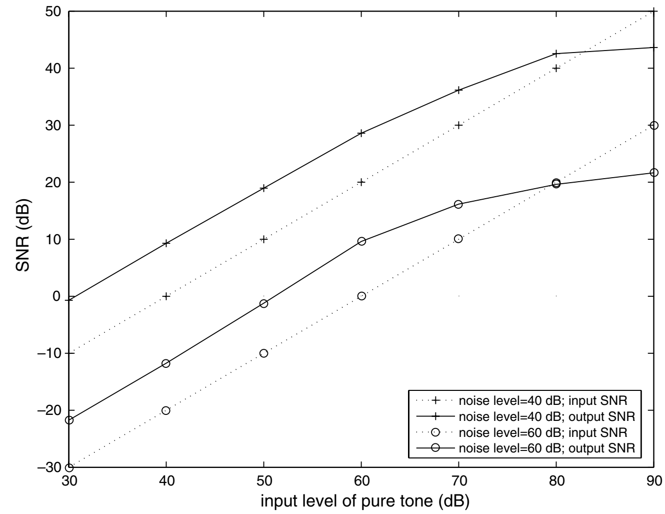

Fig. 11. Comparisons of SNRs from input and output data. The noise is broad band noise with its frequency content in [0.5, 8] kHz, and intensity (+) 40 or (○) 60 dB. The pure tone input is 2 kHz with intensity ranging from 30 to 90 dB.

see section 12.6.2 of Porat (1997). Over each interval, the function χ_i is one in a neighborhood of the center point of the interval, then falls off smoothly to zero beyond its end point(s) into a small portion of an adjacent interval.

Define the SNR in the i-th band, denoted by SNR_i, as the following:

$$\mathrm{SNR}_i = 20\log_{10}(R((u_{S+N} - u_N)\chi_i(x))/R((u_{S+N} - u_S)\chi_i(x))). \tag{16}$$

For simplicity, our input tones will take on these band center frequencies. Fig. 11 compares the two kinds of SNRs: one is the input SNR, and the other the model processed output SNR from Eq. (16) in the band of the tonal frequency. The noise is broad band with frequency content in [0.5, 8] kHz, and has intensity either 40 (+) or 60 dB (○) SPL. The pure tone input is 2 kHz with intensity ranging from 30 to 90 dB. The SNR derived from the input is linear in tone's dB intensities. The SNR from the output data, however, is shifted upward and nonlinear. The reason for this upward shift is that, even if the noise level is 40 dB at input, the noise level affecting the region near 2 kHz is suppressed by the tone and thus the output SNR is higher. This is due to the nonlinearity in our model.

Now to understand the effect of noise on gain functions, we amplify noisy sounds as follows: (1) for a given input consisting of a pure tone and a noise, solve the model in Section 2 to get u_{S+N}, u_S, and u_N; (2) derive SNR from the output by Eq. (16); (3) amplify the sound adaptively based on the SNR's.

Specifically for step (3), we use a sigmoid function to adapt the gain:

$$G_i^N = G_i/(1 + \mathrm{e}^{-w\cdot\mathrm{SNR}_i}), \tag{17}$$

where G_i is the gain obtained in Eq. (13) in the absence of noise. Note that $1/(1 + \mathrm{e}^{-w\cdot\mathrm{SNR}_i})$ is increasing from 0 to 1 as SNR_i goes from negative large to positive large. The slope of transition depends on the constant w, which is chosen as 0.5 in results reported below.

Fig. 12 shows the gain functions with and without the adaptivity in the presence of a 60 dB broad band noise with frequency content in [0.5, 8] kHz. The three rows are for the severe, moderate and mild loss, respectively, as in Fig. 9. The left column shows the gains regardless of the noise. The gains are provided as if the signals were clean. The adaptive gains are in the second column. The gain is a function of the frequency of the input pure tone, and each curve is labeled by the intensity of the pure tone ($x = 40$ dB, $\circ = 50$ dB, $* = 60$ dB, $\nabla = 70$ dB, $\square = 80$ dB, and $+ = 90$ dB). We noticed that the gain curves as a whole are lower. The two gain curves corresponding to 40 and 50 dB tones are drastically affected. The 40 dB curve is squeezed down to the bottom. The 50 dB gain curve is also sharply reduced.

Fig. 13 compares the gains for the three different hearing loss levels in the presence of low and high frequency noises. The noise in the first column is a low frequency banded noise with its spectral energy mostly supported from 0.5 to 2 kHz. The noise in the second column is a high frequency banded noise with its spectral energy mostly supported from 2 to 8 kHz. The noise level is 60 dB. We see that the gain curves labeled as 40 and 50 dB are significantly reduced in the low frequency range [0.5, 2] kHz, yet much less in the high frequency range. Similarly, the high frequency noise influences the gain curves in the high frequency range [2, 8] kHz, though the modifications are

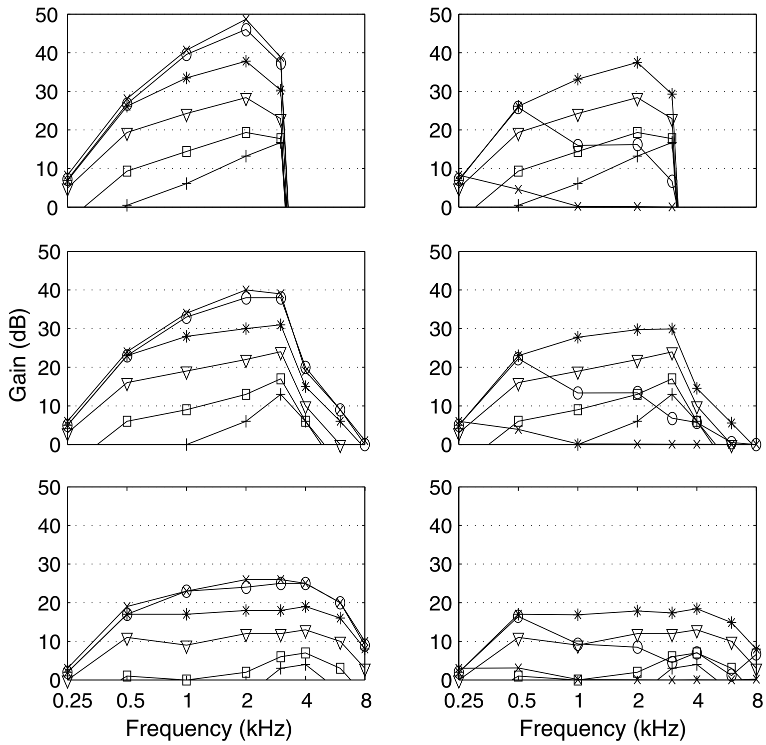

Fig. 12. Comparison of the two amplification strategies in a noisy environment: blind amplification (first column) where gains are provided as if noise were not present, and adaptive amplification with gains based on the SNR. The noise is broad band at 60 dB with spectral energy mostly supported from 0.5 to 8 kHz. The rows represent the same degrees of hearing loss as in Fig. 9. The gains are plotted as functions of the input tonal frequency, and are labeled with tone dB intensity ($x = 40$, $\bigcirc = 50$, $* = 60$, $\nabla = 70$, $\square = 80$, and $+ = 90$ dB).

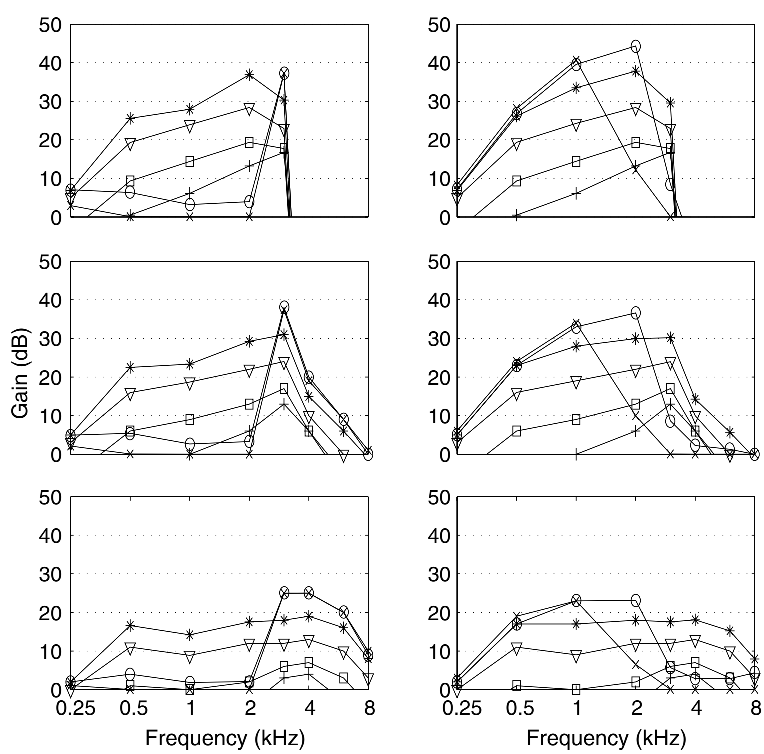

Fig. 13. Comparison of the adaptive gain functions labeled the same as in Fig. 12 for the three different hearing loss levels in the presence of low and high frequency noises. The noise in the first column is a low frequency banded noise with its spectral energy mostly supported from 0.5 to 2 kHz. The noise in the second column is a high frequency banded noise with its spectral energy mostly supported from 2 to 8 kHz. The noise level is 60 dB.

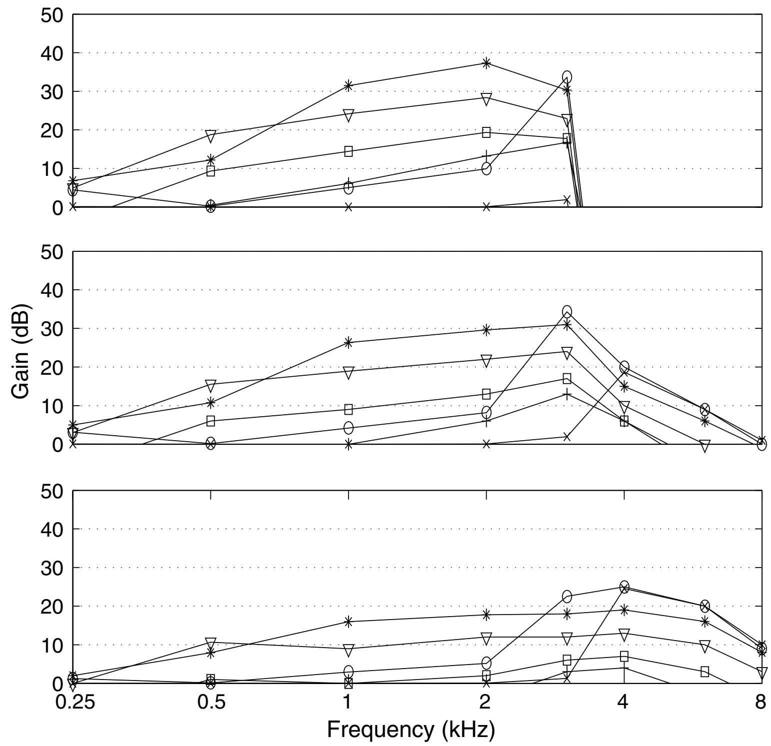

Fig. 14. Comparison of the adaptive gain functions labeled the same as in Fig. 12 for the three different hearing loss levels in the presence of 60 dB road noise. The spectral energy of the road noise is mostly in the low frequency range.

smaller, as the full gains in the high frequency range are minimal even for clean signals (Fig. 9). Fig. 14 shows the adaptive gains in the presence of a realistic 60 dB road noise whose spectral energy is mostly in the low frequency range. Fig. 14 resembles the left column of Fig. 13.

5. Discussions and conclusions

We presented a hearing aid prescription method by combining peripheral ear model and a perceptive correction motivated by speech intelligibility. The peripheral model is a two space dimensional cochlea model equipped with OHC active nonlinear compression. The model describes common characteristics of impaired ears due to OHC damage, such as raised hearing thresholds, loudness recruitment, and loss of frequency selectivity.

Our method generates gain functions with wide range dynamic compression, in agreement with those by NAL-NL1. The model computations are however not fast enough for real time purpose, hence a simplified computational algorithm must be developed for implementation with a hearing aid hardware. The other aspect is to improve the model by including a module of higher auditory pathways so that the intelligibility factor can be better approximated without additional weighting of the model output.

Our method can also be used to study adaptive gains for noisy sounds based on signal to noise ratios calculated from the model. Because gains are biased towards the signal content, the total energy of signal portion of a sound mixture across all channels is more enhanced than that of the noise portion. The overall signal to noise ratio is higher. As a result, it has the potential to increase the intelligibility. The adaptive gains depend on the frequency content and intensity of noise as Figs. 12–14 showed. Quantitative assessment of intelligibility will be studied by human listening tests in the future.

Acknowledgements

The work was partially supported by NSF Grant ITR-0219004 (J.X.) and NIH Grant 2R43DC005678-02A1 (Y.Q.). Y.K. acknowledges the ICES postdoctoral fellowship at the University of Texas at Austin. J.X. acknowledges a fellowship from the John Simon Guggenheim Memorial Foundation. The authors thank Prof. J. Keller for his interest and helpful suggestions, and the anonymous referees for their constructive comments.

References

ANSI, 1997. American National Standard Methods for Calculation of the Speech Intelligibility Index. American National Standard Institute, Inc., New York.

Ching, T., Dillon, H., Byrne, D., 1998. Speech recognition of hearing-impaired listeners: predictions from audibility and the limited role of high-frequency amplification. Journal of the Acoustical Society of America 103, 1128–1140.

Ching, T., Dillon, H., Katsch, R., Byrne, D., 2001. Maximizing effective audibility in hearing aid fitting. Ear and Hearing 22 (3), 212–224.

de Boer, E., Nuttall, A., 2003. Properties of amplifying elements in the cochlea. In: Gummer, A. (Ed.), Biophysics of the Cochlea: From Molecules to Models. World Scientific, Singapore, pp. 331–342.

Dillon, H., 2001. Hearing Aid. Boomerang Press, Sydney.

Geisler, C., 1998. From Sound to Synapse. Oxford University Press, Oxford.

Greenwood, D., 1990. A cochlear frequency-position function for several species: 29 years later. Journal of the Acoustical Society of America 87, 2592–2605.

Killion, M., 1996. Talking hair cells: what they have to say about hearing aids. In: Berlin, C. (Ed.), Hair Cells and Hearing Aids. Singular Publishing Group Inc., San Diego, CA.

Kim, Y., Xin, J., 2005. A two-dimensional nonlinear nonlocal feedforward cochlear model and time domain computation of multitone interactions. SIAM Journal of Multiscale Modeling and Simulations 4 (2), 664–690.

Leveque, R., Peskin, C., Lax, P., 1988. Solution of a two-dimensional cochlea model with fluid viscosity. SIAM Journal of Applied Math 48 (1), 191–213.

Lim K., 2000. Physical and Mathematical Cochlear Models. PhD thesis, Department of Mechanical Engineering, Stanford University.

Lim, K., Steele, C., 2002. A three-dimensional nonlinear active cochlear model analyzed by the WKB-numeric method. Hearing Research 170, 190–205.

Moore, B., 2000. Cochlear Hearing Loss. Whurr Publishers Ltd., London.

National Acoustic Labs, NAL-NL1 software, 2003.

Neely, S., 1985. Mathematical model of cochlear mechanics. Journal of the Acoustical Society of America 78 (1), 345–352.

Oxenham, A., Bacon, S., 2003. Cochlear compression: perceptual measures and implications for normal and impaired hearing. Ear and Hearing 24 (5), 352–366.

Pickles, J., 1988. An Introduction to the Physiology of Hearing, second ed. Academic Press, London.

Porat, B., 1997. A Course in Digital Signal Processing. Wiley, Inc., London.

Robles, L., Ruggero, M., 2001. Mechanics of the mammalian cochlea. Physiological Review 81 (3), 1305–1352.

Ruggero, M., Rich, N., Recio, A., Narayan, S., Robles, L., 1997. Basilar membrane responses to tones at the base of the chinchilla cochlea. Journal of the Acoustical Society of America 101 (4), 2151–2163.